

The Ratio of Ortho- to Para-H₂ in Photodissociation Regions

Amiel Sternberg^{1,2} and David A. Neufeld³

¹ School of Physics and Astronomy, Tel Aviv University, Ramat Aviv 69978, Israel

² Department of Astronomy, University of California, Berkeley, CA, 94720-3411

³ Department of Physics & Astronomy, The Johns Hopkins University, 3400 North Charles Street, Baltimore, MD 21218

Subject headings: ISM: molecules – infrared: ISM: lines and bands – molecular processes

ABSTRACT

We discuss the ratio of ortho- to para-H₂ in photodissociation regions (PDRs). We draw attention to an apparent confusion in the literature between the ortho-to-para ratio of molecules in FUV-pumped vibrationally *excited* states, and the *total* H₂ ortho-to-para abundance ratio. These ratios are not the same because the process of FUV-pumping of fluorescent H₂ emission in PDRs occurs via *optically thick* absorption lines. Thus, gas with an equilibrium ratio of ortho- to para-H₂ equal to 3 will yield FUV-pumped vibrationally excited ortho-to-para ratios smaller than 3, because the ortho-H₂ pumping rates are preferentially reduced by optical depth effects. Indeed, if the ortho and para pumping lines are on the “square root” part of the curve-of-growth, then the expected ratio of ortho and para vibrational line strengths is $3^{1/2} \sim 1.7$, close to the typically observed value. Thus, contrary to what has sometimes been stated in the literature, most previous measurements of the ratio of ortho- to para-H₂ in vibrationally excited states are entirely consistent with a total ortho-to-para ratio of 3, the equilibrium value for temperatures greater than 200 K. We present an analysis and several detailed models which illustrate the relationship between the total ratios of ortho- to para-H₂ and the vibrationally excited ortho-to-para ratios in PDRs. Recent *Infrared Space Observatory (ISO)* measurements of pure rotational and vibrational H₂ emissions from the PDR in the star-forming region S140 provide strong observational support for our conclusions.

1. Introduction

Infrared (IR) vibrational and rotational emission lines of molecular hydrogen (H_2) have been observed in a wide range of interstellar environments, including molecular clouds in star-forming regions, Herbig-Haro objects, reflection nebulae, and planetary nebulae. H_2 emission lines have also been observed in many starburst galaxies, and active galactic nuclei. Two principal sources of such emissions are (1) photodissociation regions (PDRs) where the molecules are vibrationally excited by far-ultraviolet (FUV) pumping or collisionally excited in gas heated by FUV radiation; and (2) shocked regions, in which the hydrogen molecules are collisionally excited in hot gas behind the shock waves. Observations of the rich H_2 vibrational spectrum yield line ratios that are valuable probes of the physical conditions within the emitting source: the relative strengths of the $v=1-0$ and $v=2-1$ bands, for example, allow fluorescent excitation produced by FUV-pumping to be distinguished from collisional excitation (Black & Dalgarno 1976; Black & van Dishoeck 1987; Sternberg 1988; Sternberg & Dalgarno 1989; Burton, Hollenbach & Tielens 1990; Draine & Bertoldi 1996).

The relative strengths of emissions from ortho- and para- H_2 molecules have been the subject of intensive observational investigation. In outflow regions where shock excitation is the primary emission mechanism, observations of vibrational emission lines typically reveal ortho-to-para ratios for vibrationally-excited states that are comparable to 3 (Smith, Davis & Lioure 1997), as expected if the gas behind such shocks has a ratio of ortho- to para- H_2 in local thermodynamic equilibrium (LTE) at high temperature ($T \gtrsim 200$ K).¹ PDRs, by contrast, often exhibit ortho-to-para ratios for vibrationally excited states that are smaller than 3, with typical values in the range 1.5 – 2.2 (Hasegawa et al. 1987, Ramsay et al. 1993, Chrysostomou et al. 1993, Hora & Latter 1996; Shupe et al. 1998).

In this paper we re-examine the interpretation of the ortho-to-para ratios for H_2 in PDRs. Previous discussions have failed to make a critical distinction between (1) the ortho-to-para ratio for vibrationally excited states populated by FUV-pumping; and (2) the true ortho-to-para abundance ratio, which is generally dominated by molecules in the ground vibrational state. In §2 we present a brief review of H_2 excitation in PDRs. We then argue that the ortho-to-para ratio for vibrationally excited H_2 molecules in PDRs is generally not equal to the true ortho-to-para ratio, because the process of FUV-pumping occurs via *optically thick* absorption lines and the ortho pumping rates are therefore preferentially reduced by larger transition optical depths. In §3 we present several detailed model computations which illustrate the behavior of the ortho-to-para

¹Note, however, that recent observations of *pure rotational* emissions from the outflow source HH 54 (Neufeld, Melnick & Harwit 1998) imply a non-equilibrium ortho-to-para H_2 abundance ratio ~ 1.2 in gas of temperature of 650 K. The observed ratio of ortho- to para- H_2 in HH 54 is believed to be the remnant of an earlier phase in the thermal history of the gas when the temperature was $\lesssim 90$ K. As far as we are aware, HH 54 is the *only* astronomical source observed to date in which the total ratio of ortho- to para- H_2 is demonstrably different from the expected LTE value.

ratios in PDRs for a range of conditions. In §4 we analyze recent *Infrared Space Observatory (ISO)* observations of the PDR in the star-forming region S140 which provide strong support for our conclusions. In §5 we present a discussion and summary.

2. Theory

2.1. H₂ in PDRs

PDRs are produced at the boundaries of molecular clouds which are exposed to FUV radiation fields ($\sim 6 - 13.6$ eV). The incident radiation heats the gas, and drives the cloud chemistry via photodissociation of molecules and photoionization of trace species. Recent reviews of observational and theoretical studies of PDRs have been presented by Hollenbach & Tielens (1997, 1998) and Sternberg (1998).

Photodissociation and FUV-pumping of hydrogen molecules are critical processes in PDRs. At the cloud edges the H₂ molecules are photodissociated rapidly, and the hydrogen gas is mainly atomic. The FUV radiation is attenuated with increasing cloud depth, and eventually photodissociation becomes slow compared to grain-surface H₂ formation, and the hydrogen becomes molecular. In equilibrium clouds, molecular destruction is balanced by formation at every location, and

$$Dn(\text{H}_2) = Rnn(\text{H}) \quad (1)$$

where $n(\text{H})$ and $n(\text{H}_2)$ are the local atomic and molecular hydrogen volume densities (cm^{-3}), $n = n(\text{H}) + 2n(\text{H}_2)$ is the total density of hydrogen nuclei, R is the grain-surface H₂ formation rate coefficient ($\text{cm}^3 \text{s}^{-1}$) and D is the local H₂ photodissociation rate (s^{-1}). At each point in the cloud the populations of H₂ molecules in specific vibrational and rotational levels (identified by the quantum numbers v and j) are determined by the competing processes of FUV-pumping, molecular formation, collisional excitation and de-excitation, and radiative decay.

H₂ photodissociation and FUV-pumping occur via the absorption of Lyman and Werner band photons in electronic transitions from the $X^1\Sigma_g^+$ ground state to the excited $B^1\Sigma_u^+$, $C^1\Pi_u^+$, and $C^1\Pi_u^-$ states. These excitations are followed by rapid spontaneous radiative transitions to the continuum and to bound vj levels of the ground electronic state. The transitions to the continuum lead to dissociation. The FUV-pumped molecules decay in a cascade of radiative quadrupole vibrational transitions which produces the characteristic spectrum of near-red and infrared fluorescent emission lines observed in PDRs (Black & Dalgarno 1976; Black & van Dishoeck 1987; Sternberg 1988; Neufeld & Spaans 1996; Draine & Bertoldi 1996).

The Lyman and Werner band absorption lines are expected to become optically thick in PDRs, and the molecules are then said to “self-shield”. The typical absorption line becomes optically thick at an H₂ column density of $\sim 10^{14} \text{ cm}^{-2}$, which is much smaller than the hydrogen column of $\sim 5 \times 10^{20} \text{ cm}^{-2}$ at which FUV dust-opacity becomes significant for normal interstellar

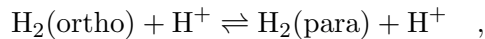
gas-to-dust ratios. Indeed, because the strongest FUV absorption lines become saturated at H_2 columns $\gtrsim 10^{17} \text{ cm}^{-2}$, these lines lie on the square-root part of the curve-of-growth throughout most of the PDR and FUV pumping and photodissociation are initiated by absorptions in the “damping wings” of the lines. At sufficiently large cloud depths the FUV-pumping and photodissociation rates become negligibly small due to the combined effects of dust-opacity and overlap of the broadest absorption lines (Tielens & Hollenbach 1985; Sternberg 1988; Draine & Bertoldi 1996).

Collisions play a critical role in the excitation of the lowest lying j -levels of the ground ($v = 0$) vibrational state. The most important are inelastic collisions with other H_2 molecules, hydrogen atoms, and protons. In high-density clouds the vj level populations of vibrationally excited molecules are influenced by collisional processes $\text{H} + \text{H}_2(vj) \rightarrow \text{H} + \text{H}_2(v'j')$ and $\text{H}_2 + \text{H}_2(vj) \rightarrow \text{H}_2 + \text{H}_2(v'j')$ which induce vibrational energy transfers. The relative intensities of the resulting H_2 emission lines differ in high density clouds because such collisional processes become more effective relative to radiative decay with increasing cloud density (Sternberg & Dalgarno 1989; Burton, Hollenbach & Tielens 1990; Draine & Bertoldi 1996).

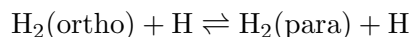
Molecular formation can also influence the populations in excited vj states. Although in equilibrium PDRs only one molecular formation event occurs for every ~ 9 FUV-pumping excitations, formation can dominate the excitation of molecules in specific vj levels that are not directly populated by FUV-pumping.

2.2. Ortho-to-Para Ratio

The ratio of ortho- to para- H_2 is a critical parameter in PDRs. We recall that ortho- H_2 possesses a total nuclear spin of 1 and exists only in states of odd rotational quantum number, while para- H_2 has a zero total nuclear spin and is represented only by states of even j . Ortho- and para- H_2 are not interconverted by any radiative process. In particular, the Lyman and Werner band transitions and the quadrupole ro-vibrational transitions which occur in PDRs cannot induce ortho-para conversions. Following the formation of H_2 in each of the ortho and para modifications, conversions can occur in the gas via “spin exchange” collisions. In cold ($T \lesssim 100 \text{ K}$) gas the ortho-para conversion occurs slowly via collisions with protons (Dalgarno, Black & Weisheit 1973; Flower & Watt 1987)



where in PDRs a small proton abundance is maintained by cosmic-ray or X-ray ionization (Sternberg & Dalgarno 1995; Maloney, Hollenbach & Tielens 1996). In warmer and partially dissociated gas, reactive collisions with hydrogen atoms (Martin & Mandy 1993; Tiné et al. 1997; Lepp et al. 1998)



control the ortho-para conversion. Grain surface exchange reactions are a third possible mechanism for ortho-para conversion: we exclude such reactions from further consideration, because their efficiency is quite uncertain and because they are unlikely to affect significantly the ortho to para-ratio under conditions where vibrational emissions are excited (Burton, Hollenbach & Tielens 1992).

When they are sufficiently rapid the ortho-para converting collisions with H or H⁺ drive the ortho-to-para abundance ratio to local thermodynamic equilibrium. In Fig. 1 we plot the LTE ortho-to-para ratio, $\alpha(T)$, as a function of temperature (see also Figure 4 of Burton et al. 1992). For $T \gtrsim 200$ K, $\alpha = 3$. At lower temperatures the molecules are driven into the $j = 0$ (para) ground state, and α falls below 3.

The actual ortho-to-para H₂ abundance ratio in PDRs depends on the competing effects of collisions, selective photodissociation of ortho and para molecules, and the molecular formation process. Furthermore, as we will now argue, the ortho-to-para ratio of molecules in vibrationally excited states is generally *not* equal to the true ortho-to-para H₂ abundance ratio.

The behavior may be understood by considering a simplified analytic model in which FUV-pumping and photodissociation is assumed to occur via a single pair of (non-overlapping) ortho and para absorption lines. The ortho-to-para ratio is controlled by the microscopic formation and destruction processes for the ortho- and para-H₂. In equilibrium

$$D_o n_o + q(o \rightarrow p) n_x n_o = R_o n n(\text{H}) + q(o \leftarrow p) n_x n_p \quad (2)$$

and

$$D_p n_p + q(o \leftarrow p) n_x n_p = R_p n n(\text{H}) + q(o \rightarrow p) n_x n_o \quad (3)$$

where n_o and n_p are the local ortho- and para-H₂ volume densities (cm⁻³), D_o and D_p are the local dissociation rates (s⁻¹) of the ortho and para molecules, $q(o \rightleftharpoons p)$ are the rate coefficients (cm³ s⁻¹) for ortho-para conversions induced by collisions with partners with density n_x , and R_o and R_p are the ortho and para molecular formation rate coefficients. The total hydrogen density $n = n(\text{H}) + 2n(\text{H}_2)$ where $n(\text{H}_2) = n_o + n_p$. Equation (1) for the H/H₂ abundance ratio is the sum of expressions (2) and (3), where $Dn(\text{H}_2) = D_o n_o + D_p n_p$, and $R = R_o + R_p$. Because most of the hydrogen molecules are almost always in the ground vibrational state and only a very small fraction are in vibrationally excited states, D_o and D_p are dissociation rates out of the $v = 0$ level.

If ortho-para converting collisions in the $v = 0$ level are very rapid compared with either molecular formation or photodissociation then it follows from eqns. (2) and (3), and the principle of detailed balance, that the *total* ortho-to-para abundance ratio

$$\frac{n_o}{n_p} = \frac{q(o \leftarrow p)}{q(o \rightarrow p)} = \alpha(T_{gas}) \quad (4)$$

and the ortho-to-para ratio is driven to LTE. The detailed numerical calculations presented in §3 and §4 below suggest that the case of rapid ortho-para conversion amongst the $v = 0$ states does

indeed apply throughout most of the PDR under most conditions of astrophysical interest. It is nevertheless instructive to consider the opposite limit in which ortho-para conversion is negligibly slow.

If ortho-para converting collisions are slow ($q = 0$) then

$$\frac{n_o}{n_p} = \frac{R_o D_p}{R_p D_o} = \frac{D_p}{D_o} \alpha(T_{form}) \quad (5)$$

where T_{form} is the formation temperature.² When the FUV absorption lines are optically thin, then $D_p/D_o = 1$ and the total ortho-to-para ratio equals $\alpha(T_{form})$. However, as the absorption lines become optically thick, D_p/D_o can become very large, or very small, depending on which set of ortho or para absorption lines first become optically thick. For absorption lines on the damping wings $D_p/D_o = (N_p/N_o)^{-1/2}$, where N_o and N_p are the total column densities of ortho and para molecules, and equation (5) can be written as the differential equation

$$\frac{dN_o}{dN_p} \equiv \frac{n_o}{n_p} = \alpha(T_{form}) \left(\frac{N_o}{N_p} \right)^{1/2} . \quad (6)$$

If $\alpha(T_{form})$ is constant through the PDR it follows that

$$\frac{n_o}{n_p} = \frac{N_o}{N_p} = \alpha^2(T_{form}) . \quad (7)$$

Thus, when ortho-para converting collisions are ineffective, preferential shielding of the ortho or para molecules maintains an ortho-to-para abundance ratio equal to the *square* of the value set by molecular formation.

We now consider the ortho-to-para ratio for vibrationally excited states. In the spirit of the two-line approximation used to treat the FUV-pumping and photodissociation in our simplified analytic model, we lump all possible vibrationally-excited states into just two states, one representing vibrationally-excited ortho-H₂ and one representing vibrationally-excited para-H₂.

If ortho-para conversion *amongst vibrationally-excited states* were rapid relative to other relevant processes (as is usually the case for ortho-para conversion for $v = 0$ molecules), then the ortho-to-para ratio in vibrationally-excited states would also equal the LTE value, $\alpha(T_{gas})$. However, when FUV-pumping dominates the molecular excitation, ortho-para conversion amongst vibrationally-excited states is generally slow, leading to more interesting behavior.

We assume that the vibrationally excited ortho- and para-H₂ molecules are populated by FUV pumping, and are removed by quadrupole decay. This is the limit of “radiative fluorescent H₂ emission” (Sternberg & Dalgarno 1989), which applies when (1) collisional excitation is

² Here we make the simplifying (though not necessary) assumption that the grain surface formation process produces the H₂ in an LTE population distribution characterized by a formation temperature T_{form} , leading to an ortho-to-para ratio $\alpha(T_{form})$.

negligible relative to FUV-pumping; and (2) when collisional de-excitation and photodissociation are negligible removal mechanisms relative to spontaneous radiative decay.

In equilibrium

$$n_o^* = P_o n_o / A \quad (8)$$

and

$$n_p^* = P_p n_p / A \quad (9)$$

where n_o^* and n_p^* are the volume densities of vibrationally excited ortho- and para-H₂, P_o and P_p are the ortho and para FUV-pumping rates, and A is the quadrupole radiative decay rate (which does not depend on the ortho or para character of the molecule). The sum of these expressions is the formation-destruction equation for vibrationally excited molecules

$$n^* = P n(\text{H}_2) / A \quad (10)$$

where n^* is the total density of vibrationally excited molecules, and P is the total (net) FUV-pumping rate.

It follows from (8) and (9) that

$$\frac{n_o^*}{n_p^*} = \frac{P_o n_o}{P_p n_p} \quad (11)$$

For absorption lines on the damping wings, $P_o/P_p = (N_o/N_p)^{-1/2}$, so that

$$\frac{n_o^*}{n_p^*} = \frac{n_o}{n_p} \left(\frac{N_o}{N_p} \right)^{-1/2} \quad (12)$$

If the true ortho-to-para ratio n_o/n_p is in LTE and is equal to a fixed value $\alpha(T_{gas})$, then $N_o/N_p = n_o/n_p$, and

$$\frac{N_o^*}{N_p^*} = \left(\frac{N_o}{N_p} \right)^{1/2} = \sqrt{\alpha(T_{gas})} \quad (13)$$

If collisional processes are unable to maintain the true ortho-to-para ratio in LTE, it follows from eqns. (5) and (11), and the fact that $P_o/D_o = P_p/D_p$ are constant molecular branching ratios,³ that the vibrationally excited ortho-to-para ratio

$$\frac{n_o^*}{n_p^*} = \alpha(T_{form}) \quad (14)$$

It then follows from eqn. (12) that

$$\frac{N_o}{N_p} = \left(\frac{N_o^*}{N_p^*} \right)^2 = \alpha^2(T_{form}) \quad (15)$$

³We note that the Lyman and Werner band transition oscillator strengths do not depend on the ortho or para character of the H₂ molecule.

assuming $\alpha(T_{form})$ is constant through the PDR.

Equations (13) and (15) represent the key result of our paper. They show that when collisional processes are ineffective at thermalizing the ortho-to-para ratio in vibrationally *excited* states, then in the limit of radiative fluorescent H₂ emission this ratio will roughly equal the *square root* of the true ortho-to-para abundance ratio. In particular, if the ($v = 0$) ortho-to-para abundance ratio is everywhere equal to an LTE value of 3, the vibrationally excited ortho-to-para ratio will tend to a non-LTE value of $\sqrt{3} \approx 1.7$, because of the lower rates of FUV-pumping in the optically thicker ortho absorption lines. Alternatively, if ortho-para interconversion of the $v = 0$ molecules is inefficient then the vibrationally excited ortho-to-para ratio is fixed by the molecular formation process. If the ortho-to-para ratio set by formation is equal to 3, the ortho-to-para abundance ratio will then tend at large cloud depths to a non-LTE ratio of 9, due to selective self-shielding of the ortho H₂.

Equations (13) or (15) describe the relationship between the vibrationally excited and total ortho-to-para ratios for the case of radiative fluorescent H₂ emission where FUV-pumping dominates the vibrational excitation and the excited molecules are removed by radiative decay. However, in dense ($n \gtrsim 5 \times 10^4 \text{ cm}^{-3}$) clouds exposed to intense FUV-fields ($\gtrsim 10^4$ times the intensity of the mean interstellar field) the PDRs can become hot ($T_{gas} \gtrsim 1000 \text{ K}$), and collisional excitation rather than FUV-pumping then dominates the vibrational excitation, particularly of $v = 1$ molecules (Sternberg & Dalgarno 1989; Burton et al. 1990). Under these conditions the vibrationally excited ortho-to-para ratio will equal the true ortho-to-para ratio since the optical depth effects associated with FUV-pumping do not apply. Ortho-para conversion is expected to be rapid in hot PDRs so the vibrationally excited ortho-to-para ratio for the collisionally excited molecules will tend to the LTE value of 3. The observations indicate that most PDRs are generally either in the limit of radiative fluorescent H₂ emission for which equations (13) and (15) apply, or are those which are hot enough to produce collisionally excited vibrational H₂ emission. Nevertheless two additional limits may be considered. First, in sufficiently dense gas, the cascade of vibrational de-excitations which follows FUV-pumping can become dominated by collisional rather than radiative de-excitations (even when collisional excitation is slow). In this limit of “collisional fluorescent H₂ emission” de-excitations via H-H₂ collisions can lead to ortho-para interconversion of the vibrationally excited molecules. Second, if the FUV-field is sufficiently intense that photodissociation dominates the removal of the vibrationally *excited* molecules, the distinction between the vibrationally excited and $v = 0$ ortho-to-para ratios disappears, and the vibrationally excited ortho-to-para ratio is then also affected by the preferential self-shielding of vibrationally-excited ortho-H₂ molecules. The ortho-to-para ratio in any vibrational state (whether the ground state or an excited state) is then simply given by equation (4) if ortho-para conversion is rapid, or equation (7) if ortho-para conversion is slow.

We now present detailed model computations which illustrate the behavior of the ortho-to-para ratios in the limits described by equations (13) and (15).

3. Models

We have carried out a series of computations using an updated version of the PDR models described by Sternberg & Dalgarno (1989, 1995).

Our models consist of static, plane-parallel, semi-infinite clouds which are exposed, on one side, to isotropic FUV radiation fields. We adopt FUV fields with spectral shapes identical to the Draine’s (1978) fit to the mean interstellar field, multiplied by an intensity scaling factor χ . At each cloud depth z (cm) we solve equation (1) for the H/H₂ ratio, and compute the steady-state population densities in each of the 301 rotational and vibrational H₂ levels in the ground electronic state. In our models we adopt the level energies and quadrupole transition rates given by Wolniewicz, Simbotin & Dalgarno (1998), and we employ the Lyman and Werner band oscillator strengths and dissociation probabilities listed by Allison & Dalgarno (1970), and Stephens & Dalgarno (1972). We treat the opacity and self-shielding in each of the several hundred Lyman and Werner absorption lines using the analytic formulae provided by Federman, Glassgold & Kwan (1979). We assume a frequency independent FUV continuum dust extinction cross section per hydrogen nucleus $\sigma = 2 \times 10^{-21}$ cm² (Sternberg & Dalgarno 1995). As discussed by Tielens & Hollenbach (1985) and by Draine & Bertoldi (1996), absorption line overlap begins to significantly affect the self-shielding when the H₂ column density exceeds $\sim 3 \times 10^{20}$ cm⁻². However, at such large column densities dust opacity becomes large ($\tau \gtrsim 0.6$ for our choice of σ) and the FUV-pumping rates are in any case reduced exponentially. We therefore ignore the effects of line overlap in the models presented here.

In our models we assume that the grain surface molecular formation rate coefficient $R = 3 \times 10^{-18} T_{gas}^{1/2}$. We also assume that one third of the H₂ binding energy is released as internal rotational and vibrational excitation, in an initial LTE vj level distribution corresponding to a formation temperature $T_{form} = (1/3)E_{diss}/k = 1.73 \times 10^4$ K, where E_{diss} is the dissociation energy for H₂ (Black & Dalgarno 1976; Black & van Dishoeck 1987; Sternberg & Dalgarno 1989). For this choice, $\alpha(T_{form}) = 3$.

In Figs. 2–4 we display the results of three illustrative model computations. For each model we plot the atomic hydrogen fractions, $n(H)/n$, and the column densities of FUV-pumped molecules, N^*/N_{max}^* , as functions of the visual extinction A_V measured from the cloud surface. In each model the gas is fully atomic at the cloud edge, and at large cloud depths the atomic fractions become small. The column densities of vibrationally excited molecules, N^* , increase linearly with depth through the atomic layer (where the FUV-pumping and H₂ formation rates per unit volume are constant) and then approach asymptotic values, N_{max}^* , at large cloud depths where the pumping rates become vanishingly small. For each model we also plot, as functions of A_V , the local values of the total ortho-to-para abundance ratio (n_o/n_p); the ratios of the total column densities in ortho and para molecules (N_o/N_p); the local ortho-to-para ratio for vibrationally excited molecules (n_o^*/n_p^*); and the ratios of the column densities in vibrationally excited ortho and para molecules (N_o^*/N_p^*). For each model we also display “excitation diagrams” in which we

plot the values of $\log_{10}(N_{vj}/g)$ vs. E_{vj} , where N_{vj} are the total cloud column densities in each vj level, and E_{vj} and g are the level energies and statistical weights. For ortho- H_2 $g = 3(2j + 1)$, and for para- H_2 $g = 2j + 1$. For clarity only the lowest $j = 0 - 7$ rotational levels in each vibrational state are displayed in the excitation diagrams.

In all three models we adopt a total hydrogen particle density $n = 10^4 \text{ cm}^{-3}$, an FUV field intensity $\chi = 2 \times 10^3$, and assume a uniform gas temperature $T_{gas} = 500 \text{ K}$. The values of n and χ are representative of typical PDRs (Hollenbach & Tielens 1998). The gas temperature of 500 K is suggested by recent observations of pure rotational lines of H_2 in several sources including the PDR in S140 (Timmermann et al. 1996; see §4). All three of these models are in the limit of radiative fluorescent emission discussed in §2.2.

In our first model we force the rotational level populations in the ground ($v = 0$) vibrational level to LTE everywhere in the cloud. This is equivalent to assuming that collisional ortho-para conversion is everywhere much more rapid than photodissociation or molecular formation for the $v = 0$ molecules. With this assumption the ortho-to-para ratio in the $v = 0$ level is equal to exactly 3 everywhere in the cloud. In this model we make the further assumption that ortho-para interconversion does *not* occur for vibrationally excited molecules. That is, we assume that ortho-para converting collisions are slow compared to all of the other processes which populate or depopulate the vibrationally excited molecules. The results are shown in Fig. 2 which shows that the total ortho-to-para ratio (both n_o/n_p and N_o/N_p) is, in fact, everywhere very close to 3. This simply reflects the fact that the total ortho-to-para ratio is dominated by $v = 0$ molecules for which the ortho-to-para ratio is fixed at 3 by assumption. However, the vibrationally excited ortho-to-para ratio falls below 3, and at large depths approaches an asymptotic value of ~ 1.7 . The difference between the total and vibrationally excited ortho-to-para ratio is also illustrated by the excitation diagram for this model. In this model the values of $\log(N_{0j}/g)$ lie on a single straight line (with slope proportional to $1/T_{gas}$) as expected for a rotational level distribution in LTE. On the other hand, the ($j = 0 - 7$) rotational distributions for vibrationally excited ortho and para molecules are each characterized by rotational temperatures $T_{rot} \sim 1500 \text{ K}$, as is typical for fluorescent emission (e.g. Sternberg & Dalgarno 1989; Draine & Bertoldi 1996). However, the distinct ortho and para distributions in the excitation diagram are vertically displaced from one another by a factor ~ 1.7 which corresponds to the (low) non-LTE ortho-to-para ratio for the vibrationally excited molecules. This model demonstrates explicitly that an ortho-to-para ratio of ~ 1.7 in vibrationally excited states is consistent with a true LTE ortho-to-para abundance ratio of 3. This behavior is consistent with equation (13).

Next, we consider a model in which ortho-para interconversions do not occur even for $v = 0$ molecules. The results are shown in Fig. 3. The vibrationally *excited* ortho-to-para ratio is now everywhere very close to a value of 3, whereas the total ortho-to-para ratio (dominated by the $v = 0$ molecules) varies markedly through the cloud. In this model the vibrationally excited ortho-to-para ratio is set by molecular formation only (with $\alpha(T_{form}) = 3$). However, the ortho-to-para ratio for $v = 0$ molecules is also significantly affected by preferential self-shielding

of the ortho molecules. Thus, at the cloud edge, where the ortho and para FUV absorption lines are all optically thin, the total ortho-to-para ratio equals the formation value of 3. At a certain cloud depth the ($v = 0$) ortho molecules begin to self-shield, while the para molecules continue to be dissociated rapidly, and the total ortho-to-para ratio becomes large. In our model the ortho-to-para abundance ratio reaches a maximum value of ~ 500 at $A_V \sim 0.1$. At still larger cloud depths the dominant ortho and para absorption lines become saturated, and the total ortho-to-para abundance ratio approaches a value $\sim 3^2 = 9$. The excitation diagram for this model shows that the populations distributions for vibrationally excited ortho and para molecules now lie on single straight lines consistent with an ortho-to-para ratio of 3. However, the rotational level distribution for $v = 0$ molecules now display a non-LTE pattern, corresponding to the integrated ortho-to-para abundance ratio of ~ 9 . The behavior illustrated by this model is consistent with equation (15).

In the third model of this series we consider a more realistic computation in which we explicitly include ortho-para conversions via $H^+ - H_2$ and $H - H_2$ collisions, for both $v = 0$ and vibrationally excited molecules. In this model we adopted the rate coefficients computed by Gerlich (1990) for $H^+ - H_2$ collisions (see also Tiné et al. 1997), and we assumed a proton density $n(H^+) = 10^{-5}n$ in the atomic zone, decreasing to $10^{-7}n$ in the molecular zone. For the $H - H_2$ collisions we adopted the semi-classical rate coefficients computed by Lepp et al. (1998).⁴ The results are shown in Fig. 4. In this model the ortho-to-para conversion rates vary from $\sim 10^{-13}n = 10^{-9} \text{ s}^{-1}$ due to $H - H_2$ collisions in the atomic zone, to $\sim 10^{-10}n(H^+) = 10^{-13} \text{ s}^{-1}$ due to $H^+ - H_2$ collisions in the molecular zone. These rates are much smaller than the unshielded photodissociation rate $\sim 5 \times 10^{-11}\chi \text{ s}^{-1} = 10^{-7} \text{ s}^{-1}$ at the cloud surface. Thus, an intermediate cloud layer (near $A_V = 0.1$) exists in which the total ortho-to-para ratio becomes large due to preferential shielding of the ortho molecules. At still larger cloud depths the photodissociation rates are attenuated to values smaller than the ortho-para conversion rate and the local ortho-para abundance ratio is thermalized to a value of 3. The vibrationally excited molecules, on the other hand, are nowhere able to attain a thermal ratio of 3, because the radiative decay rates ($\sim 10^{-6} \text{ s}^{-1}$) are much faster than the ortho-para conversion rates. Thus, the vibrationally excited ortho-to-para ratio is set mainly by the relative rates of FUV pumping of the ortho and para molecules, and the local vibrationally excited ortho-to-para ratio, n_o^*/n_p^* , tends to a value of $3^{1/2} \approx 1.7$ due to the optically thicker ortho absorption lines. The ratio of vibrationally excited ortho and para column densities, N_o^*/N_p^* , converges to the slightly larger value of 2.2, due to the small (but non-negligible) effects of collisional ortho-para interconversions of vibrationally excited molecules in the atomic hydrogen zone. The excitation diagram for this model is very similar to the excitation diagram for the “ $v = 0$ in LTE” model shown Fig. 2. In both models, the rotational populations for the vibrationally excited ortho and para molecules form distinct and vertically displaced distributions,

⁴The Lepp et al. (1998) rate-coefficients were computed using the BKMP potential (Boothroyd et al. 1996). Martin & Mandy (1993) presented similar computations using the less accurate LSTH potential (Truhlar & Horowitz 1978).

consistent with the low and non-LTE vibrationally excited ortho-to-para ratios. The excitation diagram in Fig. 4 shows that the column densities in the lowest lying ($j \leq 4$) rotational levels of the $v = 0$ molecules are very close to LTE, but that when realistic collisional rate coefficients are assumed the higher lying rotational levels become progressively subthermally populated. This model illustrates explicitly that ortho-para conversion may typically be rapid enough to maintain an LTE ortho-to-para abundance ratio of 3 for the $v = 0$ molecules, but not for vibrationally excited molecules. The preferentially lower ortho pumping rates therefore drive the vibrationally excited ortho-to-para ratio to the non-LTE value of $\sqrt{3}$, consistent with equation (13).

4. Observations

Vibrational emissions from H_2 molecules, and ortho-to-para ratios for vibrationally excited molecules, have been observed in many PDRs. Such sources include the reflection nebulae NGC 2023 and NGC 7023 (Gatley et al. 1987; Hasegawa et al. 1987; Martini, Sellgren & Hora 1997), the planetary nebulae Hubble 12, NGC 7027 and BD+30°3639 (Tanaka et al. 1989; Ramsay et al. 1993; Hora & Latter 1996; Luhman & Rieke 1996; Shupe et al. 1998), PDRs in the star-forming region M17 (Chrysostomou et al. 1993 et al.), the bipolar outflow DR21 (Fernandes, Brand & Burton 1997), and the starburst galaxy NGC 253 (Harrison et al. 1998). Typically, in regions where FUV-pumping dominates the molecular excitation the vibrationally excited ortho-to-para ratios lie in the range 1.5-2.2.

Contrary to what has been implicitly assumed in much of the previous literature on this subject, our results show that the actual abundance ratio of ortho and para molecules in PDRs is not accurately represented by the ortho-to-para ratio determined from observations of the vibrational emission lines. Previous discussions have erroneously assumed that the ortho-to-para ratios inferred from such observations must be explained by actual ortho to para- H_2 ratios smaller than 3, and have invoked a variety of processes that might lead to such ratios, including the formation of H_2 with an initial ortho-to-para ratio less than 3, rapid ortho-para conversion in low-temperature gas, or warm but time-dependent PDRs in which the ortho-to-para ratio has not had sufficient time to reach its high temperature LTE value. Our results indicate that such explanations are unnecessary: most observed values of the vibrationally excited ortho-to-para ratio are entirely consistent with the assumption that the true ortho-to-para abundance ratio is in fact 3.

Recent *Infrared Space Observatory (ISO)* observations of the PDR in the star-forming molecular cloud S140 corroborate our central result. With a broad spectral coverage that is not affected by atmospheric absorption, *ISO* has allowed both vibrational emissions *and* pure rotational mid-IR transitions of H_2 to be measured from S140 (Timmermann et al. 1996). These observations show that the relative intensities of the vibrational emissions in S140 are consistent with excitation via FUV-pumping, but that the pure rotational emissions are collisionally excited in warm gas at a temperature ~ 500 K. Most importantly, the ortho-to-para ratio for vibrationally

excited molecules is observed to be significantly less than 3, whereas the pure rotational emissions reveal that the true ortho-to-para H₂ abundance ratio is equal to an LTE value of 3.

In Fig. 5 we present a model fit to the S140 data which illustrates this key observational fact. In our model we assume that $n = 10^4 \text{ cm}^{-3}$ and $\chi = 500$, and that in S140 the cloud surface is inclined to the line-of-sight by an angle θ with $\cos \theta = 0.1$. As discussed by Timmermann et al. (1996), these are the appropriate values for the gas density, incident FUV field intensity, and cloud inclination for the S140 PDR. For these parameters our model provides an excellent fit to the observed column densities of vibrationally excited molecules. In our model we also assume that the gas temperature varies as ⁵

$$T = \frac{500 \text{ K}}{1 + 9(2n(\text{H}_2)/n)^4} \quad . \quad (19)$$

For this thermal profile the gas temperature is equal to 500 K in the outer atomic layer, and falls rapidly to 50 K as the gas becomes molecular. In this model we adopt the same H-H₂ and H⁺-H₂ rate coefficients and proton abundance as in the third model presented in §3. Our S140 model provides a very good fit to the observed column densities of rotationally excited molecules in the $v = 0$ state. This suggests that in S140 the warm gas traced by the rotational emissions is confined mainly to cloud layers where the hydrogen is atomic or partially dissociated.

In our model the ortho-to-para column density ratio for vibrationally excited molecules converges to a value of 2. Fig. 5 shows that this ratio is formed in outer cloud layers where the gas temperature $\gtrsim 200$ K, and where the true ortho-to-para abundance ratio is close to the LTE value of 3. Fig. 5 shows that at cloud depths $A_V \gtrsim 0.3$ the ortho-to-para abundance ratio falls below 3 as the gas becomes cold. However, at these large cloud depths the FUV-pumping rates become vanishingly small, and the total column densities of vibrationally excited molecules are unaffected. The excitation diagram in Fig. 5 (see also Fig. 3 of Timmermann et al. 1996) displays the observed values of (N_{vj}/g) in S140 together with our model fit. The excitation diagram again shows that the ortho-to-para ratio ~ 2 in vibrationally excited states is significantly less than the true LTE value of 3 indicated by the pure rotational states. Our S140 model is similar to the models displayed in Figs. 2 and 4, and the behavior of the total and vibrationally excited ortho-to-para ratios in S140 is consistent with equation (13).

The S140 observations provide strong support for our conclusion that the ortho-to-para ratios of ~ 1.7 typically inferred from observations of FUV-pumped H₂ emissions imply that the true ortho-to-para abundance ratios in the emitting regions are equal to LTE values of 3. An LTE ortho-to-para abundance ratio less than 3 would only be indicated by a vibrationally excited ortho-to-para ratio significantly less than $\sqrt{3} \sim 1.7$

⁵Other functional forms for the thermal profile may be assumed. For example, in the model presented by Timmermann et al. (1996) the gas temperature is assumed to vary as $T = 20K + 980K/(1 + \tau^2)$, where τ is the FUV dust continuum optical depth.

In shock-heated regions or in very hot PDRs, where collisional excitation is dominant, H₂ vibrational emissions are expected to reflect the true ortho-to-para ratio. In fact, observations of H₂ vibrational emissions in shocked regions associated with protostellar outflows and Herbig Haro objects do indeed reveal vibrationally excited ortho-to-para ratios close to 3 (Smith et al. 1997). The effects of collisional excitation to $v = 1$ within a very hot PDR are elegantly demonstrated by the recent observations of the planetary nebula BD +30°3639 by Shupe et al. (1998). Spatially-resolved line ratios in this source indicate a decrease in the $v = 2 - 1$ to $v = 1 - 0$ line ratio and an increase in the ortho-to-para ratio for $v = 1$ (from a value ~ 1.7 to a value ~ 3) with decreasing distance from the central star. Both effects may be interpreted as resulting from collisional excitation to $v = 1$ in the warmest parts of the nebula lying closest to the star, and FUV-pumping of $v = 1$ molecules in the outer cooler portions of the nebula. Our analysis shows that the true ortho-to-para ratio is likely very close to 3 at *all* observed locations in this source.

5. Discussion

Several theoretical discussions of the ortho-to-para ratio in PDRs have been presented in the literature. Takayanagi, Sakimoto & Onda (1987) argued that the ortho-to-para ratio of ~ 1.7 inferred by Hasegawa et al. (1987) from observations of fluorescent H₂ emission in NGC 2023 implies that either the gas temperature T_{gas} or formation temperature T_{form} must be very low ($\lesssim 70$ K). However, as pointed out already by Black & van Dishoeck (1987), Takayanagi et al. (1987) assumed that the FUV absorption lines are optically thin, and neglected the critically important effects of molecular self-shielding. The computations of Takayanagi et al. (1987) are therefore not relevant to the interpretation of the ortho-to-para ratios in realistic PDRs. Black & van Dishoeck (1987) also noted that in their own models (which do include optical depth effects in the FUV absorption lines) low vibrational ortho-to-para ratios are obtained even when the formation temperature is large and $\alpha(T_{form}) = 3$, and suggested that their results may be due in part to different depth dependences of the ortho and para pumping rates.

More recently, Draine & Bertoldi (1996) presented detailed models of H₂ excitation and emission in PDRs, and presented explicit computations of the ortho-to-para ratios for vibrationally excited ($v = 1$) molecules for a wide range of cloud densities, FUV field intensities, and gas temperatures. Ortho-to-para ratios were obtained for the vibrational-excited states of H₂ for two sequences of models – one with the ratio $\chi/n = 0.1 \text{ cm}^3$ and another for $\chi/n = 0.01 \text{ cm}^3$ – and for each sequence results were presented for n ranging from 10^2 to 10^6 cm^{-3} , and maximum gas temperatures ranging from 200 to 800 K.

The numerical results of Draine & Bertoldi, as summarized in Fig. 17 of their paper, are fully consistent with our analysis, although the authors did not explicitly discuss the crucial distinction between the ortho-to-para ratio in vibrationally-excited states and the true ortho-to-para abundance ratio: that distinction that seems to have been misunderstood in much of the previous and subsequent literature.

Draine & Bertoldi found that for $n \lesssim 10^4 \text{ cm}^{-3}$ and $\chi \lesssim 100$, the vibrationally excited ortho-to-para ratio is always equal to a non-LTE value of 2 ± 0.2 , significantly less than 3, while at higher densities and FUV fields the ratio approaches and even exceeds the LTE value of 3. Our analysis shows that the behavior exhibited by the Draine & Bertoldi (1996) results at low n and χ is almost certainly due to the preferential reduction of the pumping rates for ortho- H_2 which as we have discussed is expected for radiative fluorescent H_2 emission.⁶ The behavior for high n and χ , by contrast, is likely due to the combined effects of collisional excitation of $v = 1$ molecules in hot gas, as well as of preferential self-shielding of vibrationally excited ortho molecules as discussed in §2 and suggested also by Draine & Bertoldi.

In conclusion, in our paper we have addressed a long standing confusion between the ortho-to-para ratio of H_2 molecules in FUV-pumped vibrationally excited states, and the actual ortho-to-para H_2 abundance ratio. We have argued that because the process of FUV-pumping in PDRs occurs via optically thick absorption lines, a typically observed ortho-to-para ratio of ~ 1.7 for FUV-pumped molecules is consistent with, and implies, an actual LTE ortho-to-para abundance ratio of 3, and is a signature of warm gas. Our conclusions are strongly supported by recent *ISO* observations of the PDR in S140.

A.S. thanks the Radio Astronomy Laboratory at U.C. Berkeley, the Center for Star Formation Studies consortium, and the German-Israeli Foundation (grant I-551-186.07/97) for support. D.A.N. gratefully acknowledges the support of NASA grant NAG5-3316.

⁶Draine & Bertoldi (1996) did not present the values of the ortho-to-para ratios for $v = 0$ molecules in their models, but our analysis suggests that these must be close to 3.

References

- Allison, A.C., & Dalgarno, A. 1970, *Atomic Data Tables*, 1, 289
- Black, J.H., & Dalgarno, A. 1976, *ApJ*, 203, 192
- Black, J.H., & van Dishoeck, E.F., *ApJ*, 1987, 322, 412
- Boothroyd, A.I., Keough, W.J., Martin, P.G., & Peterson, M.R. 1991, *J.Chem.Phys.*, 95, 4343
- Burton, M.G., Hollenbach, D.J., & Tielens, A.G.G.M. 1990, *ApJ*, 365, 620
- Burton, M.G., Hollenbach, D.J., & Tielens, A.G.G.M. 1992, *ApJ*, 399, 563
- Chrysostomou, A., Brand, P. W. J. L., Burton, M. D., & Moorhouse, A. 1993, *MNRAS*, 265, 329
- Dalgarno, A., Black, J., & Weisheit, J.C. 1973, *Ap.Lett.*, 14, 77
- Draine, B.T. 1978, *ApJS*, 36, 595
- Draine, B.T., & Bertoldi, F. 1996, *ApJ*, 468, 269
- Federman, S.R., Glassgold, A.E., & Kwan, J. 1979, *ApJ*, 227, 466
- Fernandes, A.J.L., Brand, P.W.J.L., & Burton, M.G. 1997, *MNRAS*, 290, 216
- Flower, D.R., & Watt, G.D., 1984, *MNRAS* 209, 25
- Gatley, I., et al. 1987, *ApJ*, 318, L73
- Gerlich, D. 1990, *J.Chem.Phys.*, 92, 2377
- Harrison, A., Puxley, P., Russell, A., & Brand, P. 1998, *MNRAS*, 297, 624
- Hasegawa, T., Gatley, I., Garden, R.P, Brand, P.W.J.L., Ohishi, M., Hayashi, M., & Kaifu, N. 1987, *ApJ*, 318, L77
- Hollenbach, D.J., & Tielens, A.G.G.M. 1997, *ARAA*, 35, 179
- Hollenbach, D.J., & Tielens, A.G.G.M. 1998, *Rev.Mod.Phys.* in press
- Hora, J.L., & Latter, W.B. 1996, *ApJ*, 461, 288
- Lepp, S., Tinè, S., & Dalgarno, A. 1998, in prep.
- Luhman, K.L., & Rieke, G.H. 1996, *ApJ*, 461, 298
- Luhman, M.L., Jaffe, D.T., Sternberg, A., Herrmann, F., & Poglitsch, A. 1997, *ApJ*, 482, 298
- Maloney, P., Hollenbach, D.J., & Tielens, A.G.G.M. 1996, *ApJ*, 466, 561
- Martin, P.G., & Mandy, M.E. 1993, *ApJS*, 86, 199
- Martini, P., Sellgren, K., & Hora, J.L. 1997, *ApJ*, 484, 296

- Neufeld, D.A., & Spaans, M. 1996, *ApJ*, 473, 894
- Neufeld, D.A., Melnick, G.J., & Harwit, M. 1998, *ApJ*, 506, L75
- Ramsay, S.K., Chrysostomou, A., Geballe, T.R., Brand, P.W.J.L., & Mountain, M. 1993, *MNRAS*, 263, 695
- Shupe, D.L., Larkin, J.E., Knop, R.A., Armus, L., Matthews, K., & Soifer, B.T. 1998, *ApJ*, 498, 267
- Smith, M.D., Davis, C.J., & Lioure, A. 1997, *A&A*, 327, 1206
- Sternberg, A. 1988, *ApJ*, 332, 400
- Sternberg, A. 1998, in *The Molecular Astrophysics of Stars and Galaxies*, ed. T.W. Hartquist and D.A. Williams (Oxford University Press)
- Sternberg, A., & Dalgarno, A. 1989, *ApJ*, 338, 197
- Sternberg, A., & Dalgarno, A. 1995, *ApJS*, 99, 565
- Stephens, T.L., & Dalgarno, A. 1972, *J. Quant. Spectrosc. Radiat. Transfer*, 12, 569
- Takayanagi, K., Sakimoto, K., & Onda, K., 1987, *ApJ*, 318, L81
- Tanaka, M., Hasegawa, T., Hayashi, S.S., Brand, P.W.J.L., & Gatley, I. 1989, *ApJ*, 336, 207
- Tielens, A.G.G.M., & Hollenbach, D.J. 1985, *ApJ*, 291, 722
- Timmermann, R., Bertoldi, F., Wright, C.M., Drapatz, S., Draine, B.T., Haser, L., & Sternberg, A. 1996, *A&A*, 315, L281
- Tiné, S., Lepp, S., Gredel, R., & Dalgarno, A. 1997, *ApJ*, 481, 282.
- Trulhar, D.G., & Horowitz, C.J. 1978, *J.Chem.Phys.*, 68, 2466
- van Dishoeck, E.F., and Black, J.H. 1987, *ApJ*, 322, 412
- Wolniewicz, L., Simbotin, I, & Dalgarno, A., 1998, *ApJS*, 115, 293

Figure Captions

Fig. 1 – The ratio of ortho- to para-H₂ in local thermodynamic equilibrium, $\alpha(T_{gas})$, as a function of the gas temperature, T_{gas} .

Fig. 2 – (a) Top left panel: The atomic hydrogen fraction $n(H)/n$, and the column density of vibrationally excited H₂ relative to the total column of vibrationally excited H₂ formed in the PDR, N^*/N_{tot}^* , as functions of visual extinction, A_V . The total hydrogen gas density $n = 10^4$ cm⁻³, the incident FUV radiation intensity is $\chi = 2 \times 10^3$, and the gas temperature $T_{gas} = 500$ K. In this model the rotational levels in the $v=0$ level are assumed to be in LTE everywhere in the cloud.

(b) Bottom left panel: The total and vibrationally excited ortho-to-para ratios. The dashed curves are the local ortho-to-para ratios. The solid curves are the integrated column ortho-to-para ratios.

(c) Right panels: An excitation diagram showing $\log(N/g)$ vs. E , where N are the total model column densities in each of the rotational-vibrational levels, g is the statistical weight, and E is the energy (in K) of the level.

Fig. 3 – In this model ortho-para interconversions for the $v = 0$ molecules is suppressed.

Fig. 4 – In this model realistic ortho-para conversions via $H^+ - H_2$ and $H - H_2$ collisions are included in the computations (see text).

Fig. 5 – A model for the PDR in S140, with $n = 10^4$ cm⁻³, $\chi = 500$, and inclination $\cos\theta = 0.1$.

(a) Top left panel: The atomic hydrogen fraction $n(H)/n$, and the column density of vibrationally excited H₂, N^*/N_{tot}^* , and the temperature profile T/T_{max} (see text) as functions of visual extinction, A_V .

(b) Bottom left panel: The total and vibrationally excited ortho-to-para ratios. The dashed curves are the local ortho-to-para ratios. The solid curves are the integrated column ortho-to-para ratios.

(c) Right panel: An excitation diagram showing the observed and model values of N/g . The observations are indicated by the errorbars assuming $\pm 30\%$ ISO-SWS flux calibration uncertainties (see Timmermann et al. 1996). The square symbols indicate the model values for pure rotational states, and the triangles indicate vibrationally excited states. The dashed line indicates LTE gas at 500 K.

